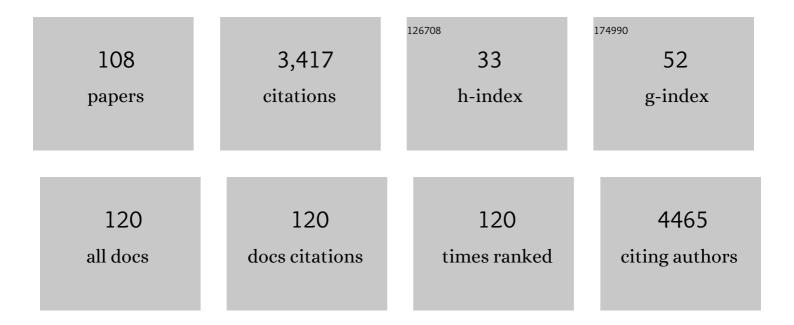
Lise Arleth

List of Publications by Year in descending order

Source: https://exaly.com/author-pdf/4642983/publications.pdf Version: 2024-02-01



#	Article	IF	CITATIONS
1	Mg2+-dependent conformational equilibria in CorA and an integrated view on transport regulation. ELife, 2022, 11, .	2.8	10
2	Global fitting of multiple data frames from SEC–SAXS to investigate the structure of next-generation nanodiscs. Acta Crystallographica Section D: Structural Biology, 2022, 78, 483-493.	1.1	3
3	Non-ionic detergent assists formation of supercharged nanodiscs and insertion of membrane proteins. Biochimica Et Biophysica Acta - Biomembranes, 2022, 1864, 183884.	1.4	2
4	Structural model of tissue factor (TF) and TF-factor VIIa complex in a lipid membrane: A combined experimental and computational study. Journal of Colloid and Interface Science, 2022, 623, 294-305.	5.0	1
5	Lipid-bound ApoE3 self-assemble into elliptical disc-shaped particles. Biochimica Et Biophysica Acta - Biomembranes, 2021, 1863, 183495.	1.4	3
6	Properdin oligomers adopt rigid extended conformations supporting function. ELife, 2021, 10, .	2.8	10
7	<i>Ab initio</i> determination of the shape of membrane proteins in a nanodisc. Acta Crystallographica Section D: Structural Biology, 2021, 77, 176-193.	1.1	4
8	Peptide discs as precursors of biologically relevant supported lipid bilayers. Journal of Colloid and Interface Science, 2021, 585, 376-385.	5.0	8
9	The microscopic distribution of hydrophilic polymers in interpenetrating polymer networks (IPNs) of medical grade silicone. Polymer, 2021, 224, 123671.	1.8	5
10	Structural and Biophysical Properties of Supercharged and Circularized Nanodiscs. Langmuir, 2021, 37, 6681-6690.	1.6	13
11	Order and disorder—An integrative structure of the full-length human growth hormone receptor. Science Advances, 2021, 7, .	4.7	25
12	Oligomerization of Pharmaceutically Relevant Insulin Analogues for Varying Concentration and Salinity Revealed by Small-Angle X-ray Scattering. Molecular Pharmaceutics, 2021, 18, 3272-3280.	2.3	0
13	Semi-empirical Analysis of Complex ITC Data from Protein–Surfactant Interactions. Analytical Chemistry, 2021, 93, 12698-12706.	3.2	6
14	Probing solution structure of the pentameric ligand-gated ion channel GLIC by small-angle neutron scattering. Proceedings of the National Academy of Sciences of the United States of America, 2021, 118,	3.3	7
15	Aescin – a natural soap for the formation of lipid nanodiscs with tunable size. Soft Matter, 2021, 17, 1888-1900.	1.2	10
16	Controlling the fractal dimension in self-assembly of terpyridine modified insulin by Fe ²⁺ and Eu ³⁺ to direct <i>in vivo</i> effects. Nanoscale, 2021, 13, 8467-8473.	2.8	3
17	Peptide Disc Mediated Control of Membrane Protein Orientation in Supported Lipid Bilayers for Surface-Sensitive Investigations. Analytical Chemistry, 2020, 92, 1081-1088.	3.2	14
18	Assessment of structure factors for analysis of small-angle scattering data from desired or undesired aggregates. Journal of Applied Crystallography, 2020, 53, 991-1005.	1.9	26

#	Article	IF	CITATIONS
19	Assembly of Capsids from Hepatitis B Virus Core Protein Progresses through Highly Populated Intermediates in the Presence and Absence of RNA. ACS Nano, 2020, 14, 10226-10238.	7.3	16
20	Orchestration of signaling by structural disorder in class 1 cytokine receptors. Cell Communication and Signaling, 2020, 18, 132.	2.7	20
21	The intracellular lipid-binding domain of human Na+/H+ exchanger 1 forms a lipid-protein co-structure essential for activity. Communications Biology, 2020, 3, 731.	2.0	11
22	A highâ€affinity, bivalent <scp>PDZ</scp> domain inhibitor complexes <scp>PICK</scp> 1 to alleviate neuropathic pain. EMBO Molecular Medicine, 2020, 12, e11248.	3.3	20
23	Structural Insight into the Self-Assembly of a Pharmaceutically Optimized Insulin Analogue Obtained by Small-Angle X-ray Scattering. Molecular Pharmaceutics, 2020, 17, 2809-2820.	2.3	3
24	Efficient refolding and reconstitution of tissue factor into nanodiscs facilitates structural investigation of a multicomponent system on a lipid bilayer. Biochimica Et Biophysica Acta - Biomembranes, 2020, 1862, 183214.	1.4	3
25	Dispersion state of TiO2 pigment particles studied by ultra-small-angle X-ray scattering revealing dependence on dispersant but limited change during drying of paint coating. Progress in Organic Coatings, 2020, 142, 105590.	1.9	13
26	Small-angle Neutron Scattering Shows that the Solution Structures of the Bacterial Mg2+-Channel CorA are Overall Similar with and without Mg2+Bound. Biophysical Journal, 2020, 118, 12a.	0.2	0
27	Combining molecular dynamics simulations with small-angle X-ray and neutron scattering data to study multi-domain proteins in solution. PLoS Computational Biology, 2020, 16, e1007870.	1.5	76
28	Protocol for Investigating the Interactions Between Intrinsically Disordered Proteins and Membranes by Neutron Reflectometry. Methods in Molecular Biology, 2020, 2141, 569-584.	0.4	2
29	Structure and dynamics of a nanodisc by integrating NMR, SAXS and SANS experiments with molecular dynamics simulations. ELife, 2020, 9, .	2.8	49
30	Title is missing!. , 2020, 16, e1007870.		0
31	Title is missing!. , 2020, 16, e1007870.		0
32	Title is missing!. , 2020, 16, e1007870.		0
33	Title is missing!. , 2020, 16, e1007870.		0
34	Aescin-Induced Conversion of Gel-Phase Lipid Membranes into Bicelle-like Lipid Nanoparticles. Langmuir, 2019, 35, 16244-16255.	1.6	22
35	PSX, Protein–Solvent Exchange: software for calculation of deuterium-exchange effects in small-angle neutron scattering measurements from protein coordinates. Journal of Applied Crystallography, 2019, 52, 1427-1436.	1.9	5
36	Circularized and solubilityâ€enhanced <scp>MSP</scp> s facilitate simple and highâ€yield production of stable nanodiscs for studies of membrane proteins in solution. FEBS Journal, 2019, 286, 1734-1751.	2.2	36

#	Article	IF	CITATIONS
37	Structure and Dynamics of the Central Lipid Pool and Proteins of the Bacterial Holo-Translocon. Biophysical Journal, 2019, 116, 1931-1940.	0.2	22
38	The influence of pH, protein concentration and calcium ratio on the formation and structure of nanotubes from partially hydrolyzed bovine α-lactalbumin. Soft Matter, 2019, 15, 4787-4796.	1.2	19
39	Distinct α-Synuclein:Lipid Co-Structure Complexes Affect Amyloid Nucleation through Fibril Mimetic Behavior. Biochemistry, 2019, 58, 5052-5065.	1.2	12
40	Towards biomimics of cell membranes: Structural effect of phosphatidylinositol triphosphate (PIP3) on a lipid bilayer. Colloids and Surfaces B: Biointerfaces, 2019, 173, 202-209.	2.5	22
41	On the Calculation of SAXS Profiles of Folded and Intrinsically Disordered Proteins from Computer Simulations. Journal of Molecular Biology, 2018, 430, 2521-2539.	2.0	64
42	Invisible detergents for structure determination of membrane proteins by smallâ€angle neutron scattering. FEBS Journal, 2018, 285, 357-371.	2.2	52
43	Comprehensive Study of the Self-Assembly of Phospholipid Nanodiscs: What Determines Their Shape and Stoichiometry?. Langmuir, 2018, 34, 12569-12582.	1.6	30
44	Introducing SEC–SANS for studies of complex self-organized biological systems. Acta Crystallographica Section D: Structural Biology, 2018, 74, 1178-1191.	1.1	42
45	Analysis of small-angle scattering data using model fitting and Bayesian regularization. Journal of Applied Crystallography, 2018, 51, 1151-1161.	1.9	16
46	Size-exclusion chromatography small-angle X-ray scattering of water soluble proteins on a laboratory instrument. Journal of Applied Crystallography, 2018, 51, 1623-1632.	1.9	36
47	Small-angle neutron scattering studies on the AMPA receptor GluA2 in the resting, AMPA-bound and GYKI-53655-bound states. IUCrJ, 2018, 5, 780-793.	1.0	9
48	Recent advances in X-ray compatible microfluidics for applications in soft materials and life sciences. Lab on A Chip, 2016, 16, 4263-4295.	3.1	91
49	Construction of Insulin 18â€mer Nanoassemblies Driven by Coordination to Iron(II) and Zinc(II) Ions at Distinct Sites. Angewandte Chemie - International Edition, 2016, 55, 2378-2381.	7.2	11
50	Construction of Insulin 18â€mer Nanoassemblies Driven by Coordination to Iron(II) and Zinc(II) Ions at Distinct Sites. Angewandte Chemie, 2016, 128, 2424-2427.	1.6	3
51	Dimeric peptides with three different linkers self-assemble with phospholipids to form peptide nanodiscs that stabilize membrane proteins. Soft Matter, 2016, 12, 5937-5949.	1.2	37
52	Formation of nanotubes and gels at a broad pH range upon partial hydrolysis of bovine α-lactalbumin. International Dairy Journal, 2016, 52, 72-81.	1.5	15
53	A de Novoâ€Designed Monomeric, Compact Threeâ€Helixâ€Bundle Protein on a Carbohydrate Template. ChemBioChem, 2015, 16, 1905-1918.	1.3	2
54	PET/CT Based In Vivo Evaluation of 64Cu Labelled Nanodiscs in Tumor Bearing Mice. PLoS ONE, 2015, 10, e0129310.	1.1	22

#	Article	IF	CITATIONS
55	Small-angle scattering determination of the shape and localization of human cytochrome P450 embedded in a phospholipid nanodisc environment. Acta Crystallographica Section D: Biological Crystallography, 2015, 71, 2412-2421.	2.5	47
56	Biosynthetic preparation of selectively deuterated phosphatidylcholine in genetically modified Escherichia coli. Applied Microbiology and Biotechnology, 2015, 99, 241-254.	1.7	31
57	Structure and crystallinity of water dispersible photoactive nanoparticles for organic solar cells. Journal of Materials Chemistry A, 2015, 3, 17022-17031.	5.2	29
58	Structure of Dimeric and Tetrameric Complexes of the BAR Domain Protein PICK1 Determined by Small-Angle X-Ray Scattering. Structure, 2015, 23, 1258-1270.	1.6	34
59	Response to The Challenges of Polydisperse SAXS Data Analysis: Two Different SAXS Studies of PICK1 Produce Different Structural Models. Structure, 2015, 23, 1969-1970.	1.6	4
60	Small-Angle X-Ray Scattering of the Cholesterol Incorporation into Human ApoA1-POPC Discoidal Particles. Biophysical Journal, 2015, 109, 308-318.	0.2	26
61	Quantification of the information in small-angle scattering data. Journal of Applied Crystallography, 2014, 47, 2000-2010.	1.9	19
62	Small-angle scattering gives direct structural information about a membrane protein inside a lipid environment. Acta Crystallographica Section D: Biological Crystallography, 2014, 70, 371-383.	2.5	58
63	A compact time-of-flight SANS instrument optimised for measurements of small sample volumes at the European Spallation Source. Nuclear Instruments and Methods in Physics Research, Section A: Accelerators, Spectrometers, Detectors and Associated Equipment, 2014, 764, 133-141.	0.7	9
64	Predicting for thermodynamic instabilities in water/oil/surfactant microemulsions: A mesoscopic modelling approach. Journal of Chemical Physics, 2014, 140, 164711.	1.2	20
65	Self-assembling peptides form nanodiscs that stabilize membrane proteins. Soft Matter, 2014, 10, 738-752.	1.2	65
66	Stealth carriers for low-resolution structure determination of membrane proteins in solution. Acta Crystallographica Section D: Biological Crystallography, 2014, 70, 317-328.	2.5	63
67	Binding of the N-Terminal Domain of the Lactococcal Bacteriophage TP901-1 CI Repressor to Its Target DNA: A Crystallography, Small Angle Scattering, and Nuclear Magnetic Resonance Study. Biochemistry, 2013, 52, 6892-6904.	1.2	12
68	Mesoscopic modelling of frustration in microemulsions. Physical Chemistry Chemical Physics, 2013, 15, 7133.	1.3	35
69	Selfâ€assembly of designed coiled coil peptides studied by smallâ€angle Xâ€ray scattering and analytical ultracentrifugation. Journal of Peptide Science, 2013, 19, 283-292.	0.8	10
70	<i>WillItFit</i> : a framework for fitting of constrained models to small-angle scattering data. Journal of Applied Crystallography, 2013, 46, 1894-1898.	1.9	61
71	Perfluoroalkyl Chains Direct Novel Self-Assembly of Insulin. Langmuir, 2012, 28, 593-603.	1.6	11
72	Metal Ion Controlled Self-Assembly of a Chemically Reengineered Protein Drug Studied by Small-Angle X-ray Scattering. Langmuir, 2012, 28, 12159-12170.	1.6	14

#	Article	IF	CITATIONS
73	Structure of Immune Stimulating Complex Matrices and Immune Stimulating Complexes in Suspension Determined by Small-Angle X-Ray Scattering. Biophysical Journal, 2012, 102, 2372-2380.	0.2	27
74	Small-angle scattering from phospholipid nanodiscs: derivation and refinement of a molecular constrained analytical model form factor. Physical Chemistry Chemical Physics, 2011, 13, 3161-3170.	1.3	57
75	Aligning Nanodiscs at the Air–Water Interface, a Neutron Reflectivity Study. Langmuir, 2011, 27, 15065-15073.	1.6	18
76	Automated microfluidic sample-preparation platform for high-throughput structural investigation of proteins by small-angle X-ray scattering. Journal of Applied Crystallography, 2011, 44, 1090-1099.	1.9	31
77	Reconciliation of opposing views on membrane–sugar interactions. Proceedings of the National Academy of Sciences of the United States of America, 2011, 108, 1874-1878.	3.3	126
78	Elliptical Structure of Phospholipid Bilayer Nanodiscs Encapsulated by Scaffold Proteins: Casting the Roles of the Lipids and the Protein. Journal of the American Chemical Society, 2010, 132, 13713-13722.	6.6	117
79	An analytical model for the small-angle scattering of polyethylene glycol-modified liposomes. Journal of Applied Crystallography, 2010, 43, 1084-1091.	1.9	18
80	Structure Analysis of Synaptic Vesicles by Solution Small-Angle Scattering of X-Rays. Biophysical Journal, 2010, 98, 284a.	0.2	0
81	Structure Parameters of Synaptic Vesicles Quantified by Small-Angle X-Ray Scattering. Biophysical Journal, 2010, 98, 1200-1208.	0.2	43
82	A new small-angle X-ray scattering set-up on theÂcrystallography beamline I711 at MAX-lab. Journal of Synchrotron Radiation, 2009, 16, 498-504.	1.0	62
83	<i>BioXTAS RAW</i> , a software program for high-throughput automated small-angle X-ray scattering data reduction and preliminary analysis. Journal of Applied Crystallography, 2009, 42, 959-964.	1.9	203
84	Interrelationship of Steric Stabilization and Self-Crowding of a Glycosylated Protein. Biophysical Journal, 2009, 97, 1445-1453.	0.2	21
85	The Effect of Glycosylation on Interparticle Interactions and Dimensions of Native and Denatured Phytase. Biophysical Journal, 2009, 96, 153-161.	0.2	15
86	3―Instead of 4â€Helix Formation in a De Novo Designed Protein in Solution Revealed by Smallâ€Angle Xâ€ray Scattering. ChemBioChem, 2008, 9, 2663-2672.	1.3	12
87	High-Throughput Small Angle X-ray Scattering from Proteins in Solution Using a Microfluidic Front-End. Analytical Chemistry, 2008, 80, 3648-3654.	3.2	88
88	Electrostastic Control of Spontaneous Curvature in Catanionic Reverse Micelles. Langmuir, 2007, 23, 9983-9989.	1.6	23
89	Block-Copolymer Micro-emulsion with Solvent-Induced Segregation. Langmuir, 2007, 23, 2117-2125.	1.6	13
90	Characterization of Prototype Self-Nanoemulsifying Formulations of Lipophilic Compounds. Journal of Pharmaceutical Sciences, 2007, 96, 876-892.	1.6	60

#	Article	IF	CITATIONS
91	Unusually large acrylamide induced effect on the droplet size in AOT/Brij30 water-in-oil microemulsions. Journal of Colloid and Interface Science, 2007, 306, 143-153.	5.0	21
92	Structural Development of Self Nano Emulsifying Drug Delivery Systems (SNEDDS) During In Vitro Lipid Digestion Monitored by Small-angle X-ray Scattering. Pharmaceutical Research, 2007, 24, 1844-1853.	1.7	109
93	Phase Behavior, Topology, and Growth of Neutral Catanionic Reverse Micelles. Langmuir, 2006, 22, 8017-8028.	1.6	20
94	Interrelationships of Glycosylation and Aggregation Kinetics for Peniophora lycii Phytase. Biochemistry, 2006, 45, 5057-5066.	1.2	39
95	Fluorescent gel particles in the nanometer range for detection of metabolites in living cells. Polymers for Advanced Technologies, 2006, 17, 790-793.	1.6	15
96	Interactions ofHumicola insolensCutinase with an Anionic Surfactant Studied by Small-Angle Neutron Scattering and Isothermal Titration Calorimetry. Langmuir, 2005, 21, 4299-4307.	1.6	33
97	Investigating the role of anionic surfactant and polymer morphology on the environmental stress cracking (ESC) of high-density polyethylene. Polymer Degradation and Stability, 2005, 89, 442-453.	2.7	20
98	Analysis of protein–surfactant interactions—a titration calorimetric and fluorescence spectroscopic investigation of interactions between Humicola insolens cutinase and an anionic surfactant. Biochimica Et Biophysica Acta - Proteins and Proteomics, 2005, 1752, 124-132.	1.1	79
99	Volume transition and internal structures of small poly(N-isopropylacrylamide) microgels. Journal of Polymer Science, Part B: Polymer Physics, 2005, 43, 849-860.	2.4	61
100	Detailed Structure of Hairy Mixed Micelles Formed by Phosphatidylcholine and PEGylated Phospholipids in Aqueous Media. Langmuir, 2005, 21, 3279-3290.	1.6	68
101	In vitro characterization of PEGylated phospholipid micelles for improved drug solubilization: Effects of PEG chain length and PC incorporation. Journal of Pharmaceutical Sciences, 2004, 93, 2476-2487.	1.6	225
102	Small-angle X-ray scattering studies of metastable intermediates of ?-lactoglobulin isolated after heat-induced aggregation. Biopolymers, 2003, 70, 377-390.	1.2	18
103	Growth Behavior of Mixed Wormlike Micelles:Â a Small-Angle Scattering Study of the Lecithinâ^'Bile Salt System. Langmuir, 2003, 19, 4096-4104.	1.6	43
104	Small-Angle Neutron Scattering Study of the Growth Behavior, Flexibility, and Intermicellar Interactions of Wormlike SDS Micelles in NaBr Aqueous Solutions. Langmuir, 2002, 18, 5343-5353.	1.6	102
105	Droplet polydispersity and shape fluctuations in AOT [bis(2-ethylhexyl)sulfosuccinate sodium salt] microemulsions studied by contrast variation small-angle neutron scattering. Physical Review E, 2001, 63, 061406.	0.8	65
106	Gaussian random fields with two level-cuts—Model for asymmetric microemulsions with nonzero spontaneous curvature?. Journal of Chemical Physics, 2001, 115, 3923-3936.	1.2	37
107	Scattering vector dependence of the small-angle scattering from mixtures of hydrogenated and deuterated organic solvents. Journal of Applied Crystallography, 2000, 33, 650-652.	1.9	13
108	Small-Angle Scattering Study of TAC8:Â A Surfactant with Cation Complexing Potential. Langmuir, 1997, 13, 1887-1896.	1.6	27